Inorg. Chem. **2007**, *46*, 10681–10692

Synchronized Fluxional Motion and Cyclometalation of Ligands in Platinum(II) Complexes

Raffaello Romeo,*,† Giuseppina D'Amico,† Emanuela Guido,† Alberto Albinati,‡ and Silvia Rizzato‡

Dipartimento di Chimica Inorganica, Chimica Analitica e Chimica Fisica, Università di Messina, Salita Sperone, 31 - Vill. S. Agata - 98166 Messina, Italy, Dipartimento di Chimica Strutturale (DCSS) e Facoltà di Farmacia, via Venezian 21, Università di Milano, Milano, Italy

Received July 13, 2007

Oscillation of the 2,9-dimethyl-1,10-phenanthroline (dmphen) ligand between nonequivalent exchanging sites in [Pt(Me)(dmphen)(P(*o*-tolyl)$_3$)]$^+$ and phosphane rotation around the Pt–P bond take place at the same rate. Thus, this cationic complex behaves as a molecular gear, exhibiting a fascinating synchronism between two otherwise independent fluxional motions. The process ($\Delta G_{333}^{\ddagger} = 68.5 \pm 0.2$ kJ mol^{-1}) was found to be unaffected by (i) the nature of various counteranions (X = PF_6^- **1**, SbF_6^- **2**, $CF_3SO_3^-$ **3**, BF_4^- **4**, BArf$^-$ **5**), (ii) the polarity or the electron-donor properties of the solvent and, (iii) the addition of weak nucleophiles. Restricted phosphane rotation around the Pt–P bond impedes free dmphen oscillation in a 14-electron three-coordinate T-shaped intermediate, containing η^1-coordinated dmphen, generated by easy Pt–N bond dissociation from [Pt(Me)(dmphen)(P(*o*-tolyl)$_3$)]$^+$. **1**–**5** undergo easy orthoplatination, leading to new [Pt(dmphen){$CH_2C_6H_4$P(*o*-tolyl)$_2$-$\kappa C,P$}]X cyclometalated Pt(II) compounds (X = PF_6^- **1**, SbF_6^- **2**, $CF_3SO_3^-$ **3**, BF_4^- **4**, BArf$^-$ **5**). The kinetics of the cyclometalation of **3** and **4** were followed in tetrachloroethane by both ^{1}H NMR and spectrophotometric techniques ($k_{obs} = 1.7 \times 10^{-4}$ s^{-1} at 333 K, $\Delta H^{\ddagger} = 59.3 \pm 3$ kJ mol^{-1}, and $\Delta S^{\ddagger} = -141 \pm 8$ J K^{-1} mol^{-1}). Ring opening of dmphen is again a prerequisite for C–H bond activation, which takes place through a multistep oxidative-addition reductive-elimination pathway. The molecular structure of cyclometalated **10** shows a butterfly shape with two *o*-tolyl rings projected above and below the coordination plane. Variable-temperature ^{1}H NMR spectra revealed hindered rotation around the P–C_{ipso}(*o*-tolyl) bonds at rather mild temperatures ($\Delta G_{333}^{\ddagger} = 55.2 \pm 0.4$ kJ mol^{-1}). Dmphen oscillation results very slowly and is dependent on the nature of the counteranions, of the solvents, and is strongly accelerated by the presence of weak nucleophiles that act as catalysts, according to an associative mode of activation.

Introduction.

Steric congestion is at the origin of the oscillation of symmetric chelating ligand 2,9-dimethyl-1,10-phenanthroline (dmphen) between nonequivalent exchanging sites in cationic complexes of the type [Pt(Me)(dmphen)(L)]$^+$, where L is a neutral sulfur or phosphorus donor ligand. Detailed kinetic and structural studies have shown that the mechanism is switchable between associative and dissociative pathways.[1−4] According to the activation mode, the electron donor properties of the solvent or of the counteranion used can or cannot affect the flipping rate. Rate accelerations can be achieved by the addition of weak external nucleophiles acting as catalysts (associative mechanism) or by the use of bulky coordinated ligands (dissociative mechanism). Application of the standard quantitative analysis of ligand effects (QALE) methodology[5] enabled a quantitative separation of steric and electronic contributions brought about by either added[2] or coordinated ligands[3] to the values of the free activation

* To whom correspondence should be addressed. E-mail: rromeo@unime.it, Phone: +39 − 090 − 6765717, Fax: +39 − 090 − 393756.
† Università di Messina.
‡ Università di Milano.

(1) Romeo, R.; Fenech, L.; Monsù Scolaro, L.; Albinati, A.; Macchioni, A.; Zuccaccia, C. *Inorg. Chem.* **2001**, *40*, 3293−3302.
(2) Romeo, R.; Fenech, L.; Carnabuci, S.; Plutino, M. R.; Romeo, A. *Inorg. Chem.* **2002**, *41*, 2839−2847.
(3) Romeo, R.; Carnabuci, S.; Plutino, M. R.; Romeo, A.; Rizzato, S.; Albinati, A. *Inorg. Chem.* **2005**, *44*, 1248−1262.
(4) Romeo, R.; Carnabuci, S.; Fenech, L.; Plutino, M. R.; Albinati, A. *Angew. Chem., Int. Ed.* **2006**, *45*, 4494−4498.
(5) http://www.bu.edu/qale. This Web site collects sets of data, protocol for the analysis, program package, parameters of ligands, leading references, etc. Each set of data, taken from the literature, is subjected to a QALE analysis with commentary on how each analysis is done and how successful it is. All of the material is updated with recent data sets and analyses.

10.1021/ic701396j CCC: $37.00
Published on Web 11/14/2007

Chart 1. Possible Structures of the Intermediates Accounting for the Synchronism of Dmphen (N_A-N_B) Flipping and Phosphane Rotation: (A) T-shaped Three-coordinate and (B) Pyramidal Five-Coordinate

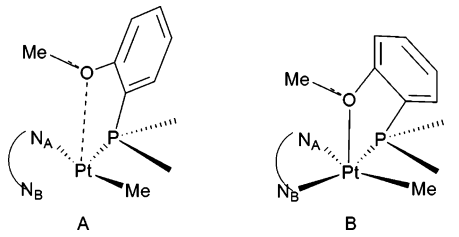

energies $\Delta G^{\ddagger}$ of the flipping motion. In particular, a free-energy surface constructed for a reacting system containing a wide series of different PR_3 phosphanes would predict a very fast flipping of dmphen when using phosphanes with a high cone angle.[3]

The nice possibility of fine-tuning rates and activation energies of these systems was prevented when dealing with overcrowded substrates. Contrary to the expectations, complexes bearing bulky *o*-methoxyphenyl groups on the phosphorus atom were found to decrease the rate of flipping of dmphen.[4] In addition, these rates were found to be identical to those of phosphane rotation around the Pt−P bond, making the system to behave as a molecular gear. The connection between the two dynamic motions appeared to be due to the impediment of dmphen oscillation by restricted phosphane rotation in a T-shaped three-coordinate intermediate, generated from Pt−N bond dissociation and containing η^1-coordinated dmphen.

The coordinative and electronic unsaturation of this 14-electron species would be somewhat compensated by temporary electronic assistance from one oxygen of a methoxy-group (structure A in Chart 1). A reasonable mechanistic alternative to dissociation could be a direct attack at the metal center by the oxygen atom of the methoxy group and an intramolecular turnstile rearrangement in a five-coordinate intermediate (structure B in Chart 1). The interest to extend the study to similar overcrowded complexes is manifold. New kinetic data can help to overcome the mechanistic ambiguity between various mechanisms, and the comprehension of the nature of the reaction intermediate opens the way to the design of molecular gears whose dynamics can be controlled by the ligand stereoelectronic properties (dissociative mechanism) or by external chemical stimuli (associative mechanism).

In this work, we show that complexes of the type [Pt(Me)(dmphen)(P(*o*-tolyl)$_3$)]X (X = PF_6^- **1**, SbF_6^- **2**, BF_4^- **4**, $BArF^-$ **5**) exhibit structural and dynamic properties entirely similar to those of the corresponding *o*-methoxy compounds, with an interesting synchronism between dmphen oscillation and phosphane rotation. In this case, the operation of a turnstile mechanism seems highly unlikely, as a result of the very low nucleophilicity of the C−H bond of the substituent methyl groups. Rather, at temperatures well above the coalescence of the monitored signals, the onset of an easy and rapid orthoplatination reaction is observed, leading to [Pt(dmphen){$CH_2C_6H_4$P(*o*-tolyl)$_2$-*κC,P*}]X complexes (**6**−**10**). The kinetics of orthoplatination (for **3** and **4**), the structure in the solid state (for **10**), and the behavior in solution of **6**−**10** were studied in detail and, aside from the usual phenanthroline fluxional motion, revealed restricted rotation around the P−C_{ipso}(*o*-tolyl) bonds.

Chart 2. Structural Formula of the Cation in **1**−**5** with Atomic Numbering

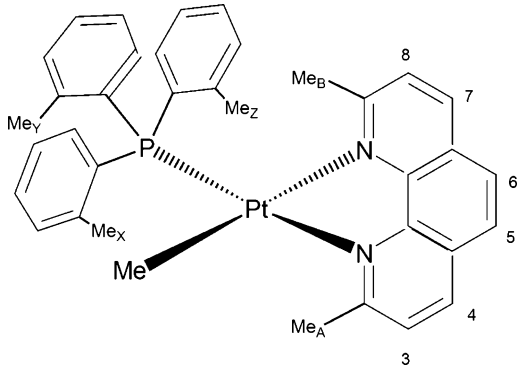

Results.

Synthesis, NMR Characterization, and Dynamic Behavior of 1−5. To synthesize different salts of the same cation [Pt(Me)(dmphen)(P(*o*-tolyl)$_3$)]$^+$, a new procedure was adopted that involves (i) removal of chloride from [Pt(Me)(dmphen)Cl] by an appropriate silver salt in a dichloromethane/methanol (20:1 ratio) mixture, (ii) separation of AgCl, and (iii) subsequent addition of stochiometric tri-*o*-tolylphosphane to the solution, according to the following sequence of substitution reactions

$$[Pt(Me)(dmphen)Cl] + AgX \xrightarrow[CH_2Cl_2/MeOH]{} [Pt(Me)(dmphen)(MeOH)]^+X^- + AgCl\downarrow + P(o\text{-tolyl})_3 \rightarrow [Pt(Me)(dmphen)(P(o\text{-tolyl})_3)]X$$

X represents a series of weakly bonding anions such as PF_6^- for **1**, SbF_6^- for **2,** $CF_3SO_3^-$ for **3,** BF_4^- for **4**, and $BArf^-$ for **5**.[6] The reaction products were isolated in high yield as solids and characterized by elemental analysis and ^{1}H and ^{31}P{^{1}H} NMR spectra. The proton resonances were assigned from the connectivities in the ^{1}H-2D NOESY spectra and on the basis of previous experiments based on scalar couplings and dipolar couplings[1] and are reported in the Experimental Section for each compound. The structural formula of the cation of the **1**−**5** salts with the atomic numbering scheme is given in Chart 2.

At 298 K in $C_2D_2Cl_4$, the NMR spectra of **1**−**5** displayed the following common features:[7] (i) A ^{31}P{^{1}H} singlet flanked by platinum satellites (δ 5.20, $^1J_{PtP}$ = 4514 Hz), (ii) a set of aromatic proton signals of the phenanthroline (δ 8.55, H_4; 8.40, H_7; 8.00, $H_{5,6}$; 7.76, H_3; 6.87, H_8), (iii) two signals for the methyl protons of the phenanthroline ligand (δ 2.95, CH_{3A}; 1.78, CH_{3B}), (iv) a set of three different

(6) Anions with good coordinating ability could not be used because they remove dmphen from the coordination sphere of the metal.
(7) Specific values reported in the text for δ, $^1J_{PtP}$, and $^2J_{PtH}$ refer to **1**.

Table 1. Counterion, Solvent, and Nucleophile Dependence of the Synchronized Rates of Flipping Motion of 2,9-Dimethyl-1,10-phenanthroline and of Phosphane Rotation in the Cationic Complex [Pt(Me)(dmphen)(P(*o*-tolyl)$_3$))]$^{+}$ [a]

complex	X	solvent	[Me_2S] mM	k_{333} (s^{-1})	$\Delta H^{\ddagger}$ (kJ mol^{-1})	$\Delta S^{\ddagger}$ ($JK^{-1}mol^{-1}$)	$\Delta G^{\ddagger}_{333}$ (kJ mol^{-1})
1	PF_6	$C_2D_2Cl_4$		139.0	55.7 ± 1.1	−37.7 ± 3.6	68.3 ± 0.1
2	SbF_6	$C_2D_2Cl_4$		121.8	56.1 ± 2.3	−37.6 ± 7.1	68.6 ± 0.1
3	CF_3SO_3	$C_2D_2Cl_4$		118.9	55.1 ± 3.6	−40.8 ± 11.3	68.7 ± 0.2
4	BF_4	$C_2D_2Cl_4$		117.3	49.4 ± 1.3	−58.0 ± 4.1	68.7 ± 0.1
5	BArf	$C_2D_2Cl_4$		135.6	51.9 ± 0.5	−49.3 ± 1.5	68.3 ± 0.1
1	PF_6	$CDCl_3$		140.0			
1	PF_6	Acetone-d_6		142.0			
1	PF_6	CD_3OD		130.0			
1	PF_6	$C_2D_2Cl_4$	0	19[b]			
1	PF_6	$C_2D_2Cl_4$	40	19[b]			
1	PF_6	$C_2D_2Cl_4$	110	19[b]			
1	PF_6	$C_2D_2Cl_4$	120	19[b]			
1	PF_6	$C_2D_2Cl_4$	180	19[b]			

[a] At 333 K. [b] At 305 K.

single signals for the methyl substituent groups in ortho position to the aryl rings in the phosphane ligand (δ 3.58, CH_{3Z} ; 1.50, CH_{3Y} ; 0.85, CH_{3X}), (iv) the ^{1}H NMR spectrum of **1** is completed by a multiplet for the coordinated methyl group with δ 0.59, $^2J_{PtH}$ 67.8 Hz. These observations are entirely compatible with hindered rotation around the metal−phosphorus bond. This has been suggested before for the bulky P(*o*-OMePh)$_3$ in the parent methoxy complex[4] and for other bulky phosphanes in a variety of square-planar compounds.[8] When the temperature was raised, the signals of the aromatic proton pairs H_3 and H_8, H_4 and H_7, and of the substituent methyl groups in the 2 and 9 positions of the phenanthroline showed a definite broadening, indicating a site exchange of the two nitrogen atoms of the dmphen ligand. Likewise, the expected collapse of the *o*-tolyl subspectrum was observed. Inspection of the ^{31}P NMR spectrum in a range of temperatures near the coalescence revealed the absence of broadening and of a possible phosphane dissociation. The dynamic ^{1}H NMR spectrum of **1** is reported in Figure 1.

The rate of oscillation of dmphen was monitored using as a probe the broadening of both the signals of the proton pair H_4 and H_7 and those of the methyl groups (CH_{3A} and CH_{3B}, respectively, in Figure 1). The rate of phosphane rotation was followed by monitoring the changes of the signals of the methyl protons of the *o*-tolyl groups (CH_{3X}, CH_{3Y}, and CH_{3Z}, in Figure 1). The analysis was performed by use of the computer program *gNMR 4.0*,[9] and the results of separate determinations of the rates and of the activation parameters are collected in Table SI1 in the Supporting Information.

The rate constants of both dynamic processes, determined separately as described above or by a full line-shape analysis of the spectra, were found to be practically identical in each kinetic run. The enthalpy changes, $\Delta H^{\ddagger}$, range in magnitude from 49 to 56 kJ mol^{-1}, and the entropy changes, $\Delta S^{\ddagger}$, range from −58 to −38 J K^{-1} mol^{-1}, but these values are not considered to provide any real insight into the nature of the fluxional process because of their extreme sensitivity to systematic errors associated with the line-shape analysis. The activation energies $\Delta G^{\ddagger}$ (333 K) are more meaningful.[10] A proper kinetic study of the fluxional behavior over the temperature of coalescence (347 K, Figure 1) was prevented by easy conversion of **1**−**5** into the cycloplatinated **6**−**10**. The kinetic runs were carried at different temperatures, over a range of solvents, or in the presence of added nucleophiles,

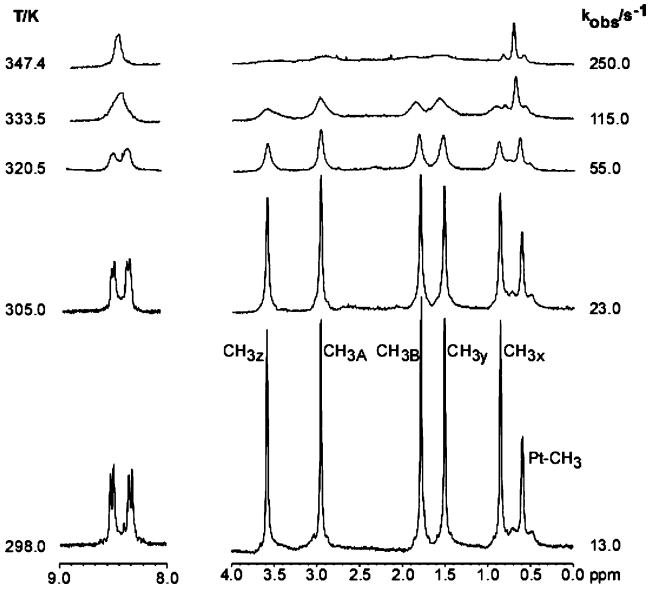

Figure 1. ^{1}H DNMR spectrum of **1** (300 MHz, $C_2D_2Cl_4$, TMS) showing the temperature dependence of the signals of the phenanthroline proton pairs H_4 and H_7, of the methyl protons CH_{3A} and CH_{3B}, and of the methyl groups of the phosphane ligand CH_{3X},CH_{3Y},CH_{3Z}.

(8) (a) Bushweller, C. H.; Rithner, C. D.; Butcher, D. J. *Inorg.Chem.* **1986**, *25*, 1610−1616. (b) DiMeglio, C. M.; Luck, L. A.; Rithner, C. D.; Rheingold, A. L.; Elcesser, W. L.; Hubbard, J. L.; Bushweller, C. H. *J. Phys. Chem.* **1990**, *94*, 6255−6263. (c) DiMeglio, C. M.; Ahmed, K. J.; Luck, L. A.; Weltin, E. E.; Rheingold, A. L.; Bushweller, C. H. *J. Phys. Chem.* **1992**, *96*, 8765−8777. (d) Crocker, C.; Goodfellow, R. J.; Gimeno, J.; Uson, R. *J. Chem. Soc., Dalton Trans.* **1977**, *15*, 1448−1452. (e) Bright, A.; Mann, B. E.; Masters, C.; Shaw, B. L.; Slade, R. M.; Stainbank, R. E. *J. Chem. Soc. A* **1971**, 1826−1831. (f) Mann, B. E.; Masters, C.; Shaw, B. L.; Stainbank, R. E. *J. Chem. Soc., Chem. Commun.* **1971**, 1103−1104. (g) Attig, T. G.; Clark, H. C. *J. Organomet. Chem.* **1975**, *94*, C49−C52. (h) Mann, B.; Musco, A. *J. Organomet. Chem.* **1979**, *181*, 439−443. (i) Empsall, H. D.; Hyde, E. M.; Mentzer, E.; Shaw, B. L. *J. Chem. Soc., Dalton Trans.* **1977**, 2285−2291. (j) Giannandrea, R.; Mastrorilli, P.; Palma, M.; Fanizzi, F. P.; Englert, U.; Nobile, C. F. *Eur. J. Inorg. Chem.* **2000**, 2573−2576. (k) Mastrorilli, P.; Nobile, C. F.; Latronico, M.; Gallo, V.; Englert, U.; Fanizzi, F. P.; Sciacovelli, O. *Inorg. Chem.* **2005**, *44*, 9097−9104. (l) Deeming, A. J.; Cockerton, B. R.; Doherty, S. *Polyhedron* **1997**, *16*, 1945−1956. (m) Pelczar, E. M.; Nytko, E. A.; Zhuravel, M. A.; Smith, J. M.; Glueck, D. S.; Sommer, R.; Incarvito, C. D.; Rheingold, A. L. *Polyhedron* **2002**, *21*, 2409−2419.

(9) *gNMR 4.0*; Cherwell Science: Oxford, U.K.

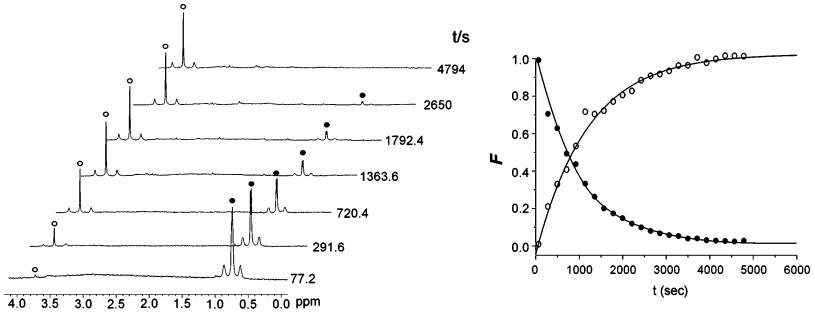

Figure 2. ^{1}H NMR (300 MHz) spectra of **3** (11.6 mm, in $C_2D_2Cl_4$) at 376.8 K as a function of time. Left plot: Pt−CH_3 signals of **3** (δ = 0.60 ppm, $^2J_{PtH}$ = 71.0 Hz); Pt−CH_2− signals of **8** (δ = 3.77 ppm, $^2J_{PtH}$ = 100 Hz); Right plot: Exponential curves for the change of the molar fraction of the two labels with time.

Scheme 1. Orthoplatination Reaction within **1**−**5**

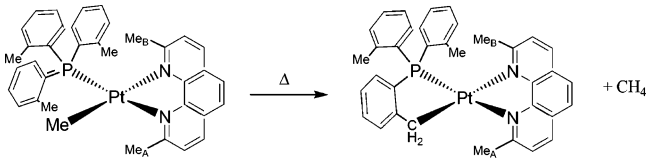

and the rates constants, calculated by a full line-shape analysis, and the associated activation parameters are given in Table 1.

Cyclometalation Kinetics. During the synthetic workup and the variable-temperature NMR experiments, we observed that phosphane-containing **1**−**5** undergo an orthoplatination reaction, leading to **6**−**10** with the liberation of methane, as shown in Scheme 1.

Products **6**−**10** were isolated as solids and characterized by elemental analysis and ^{1}H and ^{31}P NMR spectra. The spectroscopic data are given in detail in the Experimental Section. A crystal structure determination of **10** was also performed.

The temperature dependence of the cyclometalation reaction in Scheme 1 was followed in $C_2D_2Cl_4$ by ^{1}H NMR for **3** and by conventional spectrophometric techniques for **4**. There was no evidence in the ^{1}H NMR spectra for the buildup of significant amounts of any other intermediate species, and only starting **3**, cyclometalated **8**, and methane were revealed in solution. The primary kinetic data (Table SI2 in the Supporting Information) were collected, monitoring the decrease of the ^{1}H NMR signal of the coordinated methyl group in **3** and the parallel and matching increase of the methylene signal in **8**, as shown in Figure 2. The reaction goes to completion in about 2 h at 376 K. The kinetics were examined by using the time dependence of the fraction of reaction (F) of the label, obtained by integration of the signals monitored. The F versus time curve followed the simple exponential relationship expected for a first-order process (right plot in Figure 2), and the first-order rate constant k_{cy} was obtained from a nonlinear regression analysis of the equation $F_t = c_1 + c_2 \exp(-k_{cy}t)$, with c_1, c_2, and k_{cy} as the parameters to be optimized. Spectrophotometric kinetics were monitored by conventional spectrophotometry, using $C_2D_2Cl_4$ as the solvent and **4** as the starting complex. The variable-temperature rate constants obtained with the two techniques were fitted to the Eyring equation (Figure 3), leading to $\Delta H^{\ddagger} = 59.3 \pm 3$ kJ mol^{-1}, $\Delta S^{\ddagger} = -141.0 \pm 8$ J K^{-1} mol^{-1}, and $\Delta G^{\ddagger}_{333} = (106 \pm 0.2)$ kJ mol^{-1}.

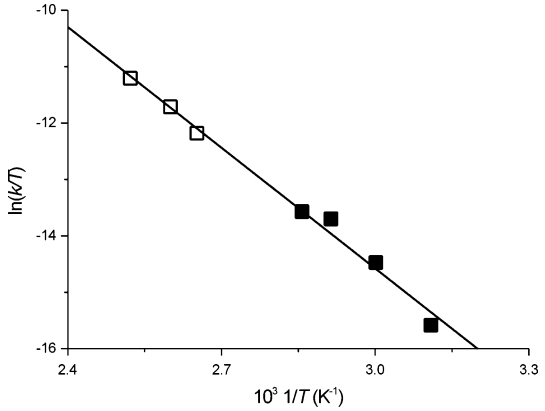

Figure 3. Eyring plot for the cyclometalation reaction in Scheme 1, constructed by the use of rate data obtained with different techniques and compounds: (Empty squares, **4**, from spectrophotometric experiments); (full squares, **3**, from ^{1}H NMR experiments).

Table 2. Selected Bond Lengths (Angstroms), Bond Angles (Degrees), and Torsion Angles (Degrees) for **10**

Pt1−P1	2.229 (1)	N1−Pt1−N2	77.4 (2)
Pt1−C17c	2.045 (5)	P1−Pt1−C17c	81.4 (1)
Pt1−N1	2.123 (4)	N1−Pt1−C17c	96.1 (2)
Pt1−N2	2.148 (4)	N2−Pt1−P1	103.2 (1)
N1−C2	1.327 (6)	N1−Pt1−P1	168.4 (1)
N1−C10	1.380 (7)	N2−Pt1−C17c	169.0 (2)
N2−C9	1.329 (7)	P1−C11c−C16−C17c	3.2 (6)
N2−C10′	1.371 (7)	Pt1−P1−C121−C122	8.2 (5)
P−C11c	1.813 (5)	Pt1−P1−C111−C112	123.4 (4)
P−C111	1.822 (5)	Pt1−P1−C11c−C16c	20.6 (4)
P−C121	1.822 (5)		

angles between least-squares defined by atoms
(dmphen)[a] ∠ (Pt1, N1, N2) 42.11 (8)
(P1−C)[b] ∠ (Pt1, N1, N2) 47.2 (1)
(C6, C5, C6′, C4′, C10, C10′). ∠ Py(1)[c] 9.71 (8)
(C6, C5, C6′, C4′C10, C10′) ∠ Py(2) 11.1 (1)

[a] dmphen refers to the least-squares planes defined by the atoms of the phenanthroline moiety, except the two methyl groups in positions 2,9. [b] Lsq plane defined by atoms P1, C17c, and those of the phenyl moiety. [c] Py(1) and Py(2) refer to the rings containing atoms N1 and N2 respectively.

X-ray Structure of 10. Selected bond distances and angles are listed in Table 2.

There are two independent molecules in the asymmetric unit; however, there are no significant differences in the coordination geometries between the two molecules. We note that the only differences ($>3\sigma$) are in the conformations of

(10) Sandström, J. *Dynamic NMR Spectroscopy*; Academic Press: London, 1982; ISBN 0−12-618620

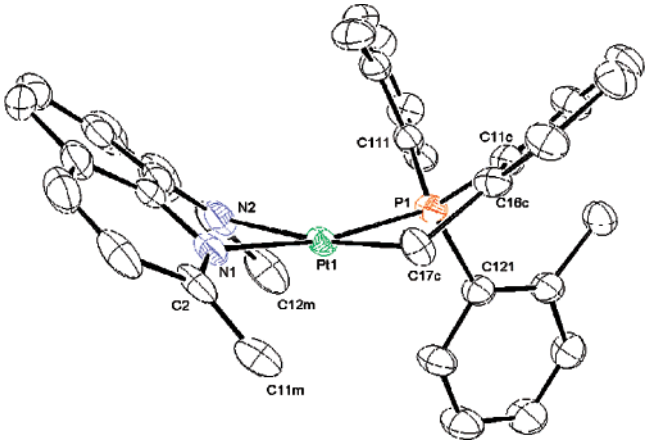

Figure 4. ORTEP view of one of the two independent molecules in **10**. Ellipsoids are drawn at 50% probability.

the phenyl rings bonded to the phosphorus atom and in the dihedral angles between the coordination plane (defined by the platinum, phosphorus, C17c, and nitrogen atoms) and those defined by the chelating ligands. As the largest differences are ca. 3 degrees, only the geometry of one of the two molecules, shown in Figure 4, will be discussed. The platinum atom is located in a tetrahedrically distorted square-planar environment defined by the two nitrogen atoms of the phenanthroline N(1) and N(2) and by the two donor atoms of the chelating ligand ($PPh_2-Ph-CH_2$-*k C,P*), with maximum deviation from the mean square plane of 0.156(2) Å for the platinum atom. The values of the bite angles for the phenanthroline N(1)−Pt(1)−N(2) and for the *kC,P* ligand P(1)−Pt(1)−C(17c) are 77.4(2) and 81.4(1)°, respectively. The Pt−C and Pt−P bond lengths (2.045(5) and 2.229(1) Å, respectively) are in the range of values reported for uncyclometalated phosphane-alkyl phenanthroline complexes of Pt(II).[1−4,11]A significant feature of the latter compounds is that the Pt−N(2) separation (i.e., that cis to the phosphorus-donor atom) shows a significant elongation with respect to the Pt−N(1) separation, caused by the concurrent strong σ donicity of the trans ligand group (the carbon atom) and the steric requirements of the phosphane ligand. These values for **10**, (Pt(1)−N(2) = 2.148 (4) Å and Pt(1)−N(1) = 2.123 (4) Å), lie toward the lowest limits of the series, suggesting only a moderate steric congestion by the $PtPh_2$ molecular fragment of the chelating ligand. The phosphorus atom exhibits a tetrahedral arrangement with the two aryl groups projecting on opposite sides of the coordination plane with different orientation, as can be judged from the the dihedral angles values for C(17c)−Pt(1)−P(1)−C(111) and C(17c)−Pt(1)−P(1)−C(121) of −143.3(2) and 91.2(2)°, respectively.

A remarkable feature of this structure is the striking tilt away from the coordination plane, in the same direction, of both the dmphen and the cyclometalated rings, making the overall molecule to look like a butterfly with asymmetric wings. The phenomenon is well-known for dmphen and is

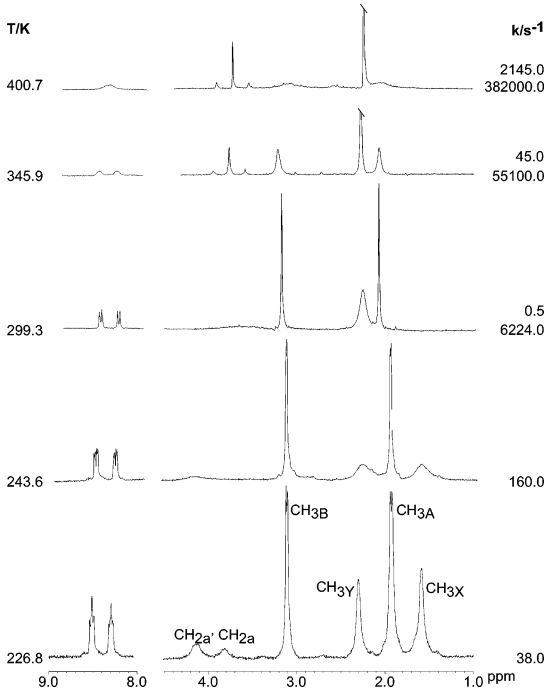

Figure 5. ^{1}H DNMR spectrum of **6** (300 MHz, $C_2D_2Cl_4$, TMS) showing the broadening of the signals of the proton pair, H_4 and H_7, of the methyl protons of the phenanthroline and of the phosphane ligand. The rates (k_{obs}, s^{-1}) refer to dmphen oscillation, upper data; aryl rotation, lower data.

steric in nature. Steric congestion brought by the methyl substituents in proximity to the other groups coordinated to the metal favors a pronounced distortion of the ligand that is observed in a number of similar X-ray structures.[1−4,12] In this case, the distortion is measured by the value of the dihedral angle, 42.11(8)°, between the plane defined by atoms Pt(1), N(1), and N(2) and that defined by the atoms of the phenanthroline (cf. Table 2). A minor concurrent effect is the loss of planarity of the ligand, as measured by the dihedral angle between the pyridyl moieties (20.9(1)°). The distortion of the cycloplatinated ring can be judged from the value of the dihedral angle, 47.2(1)°, between the plane defined by atoms Pt(1), N(1), and N(2) and that defined by the cyclometalated moiety.

Dynamic Behavior of 6−10. Key features of the static ^{1}H NMR spectra of **6**−**10** are ($C_2D_2Cl_4$, 233 K):[13] (i) A set of well-resolved signals for the aromatic protons of the phenanthroline (δ 8.52 (d, $^3J_{HH}$ = 8.8 Hz, 1H, H_4); 8.30 (d, $^3J_{HH}$ = 8.8 Hz, 1H, H_7); 7.90 (d, $^3J_{HH}$ = 8.8 Hz, 2H, $H_{5,6}$); 7.19 (d, $^3J_{HH}$ = 8.8 Hz, 1H, H_3); 7.06 (d, $^3J_{HH}$ = 8.8 Hz, 1H, H_8)) together with a group of broad signals (δ 9.65 (br,

(11) *International Tables for X-ray Crystallography*; Wilson, A. J. C., Ed.; Kluwer Academic Publishers: Dordrecht, The Netherlands, 1992; Vol.C

(12) (a) Klein, A.; McInnes, E. J. L.; Kaim, W. *J. Chem. Soc., Dalton Trans.* **2002**, 2371−2378. (b) Clark, R. J. H.; Fanizzi, F. P.; Natile, G.; Pacifico, C.; van Rooyen, C. G.; Tocher, D. A. *Inorg. Chim. Acta* **1995**, *235*, 205−213. (c) Fanizzi, F. P.; Intini, F. P.; Maresca, L.; Natile, G.; Lanfranchi, M.; Tiripicchio, A. *J. Chem. Soc., Dalton Trans.* **1991**, 1007−1015. (d) Fanizzi, F. P.; Natile, G.; Lanfranchi, M.; Tiripicchio, A.; Laschi, F.; Zanello, P. *Inorg. Chem.* **1996**, *35*, 3173−3182. (e) De Felice, V.; Albano, V. G.; Castellari, C.; Cucciolito, M. E.; De Renzi, A. *J. Organomet. Chem.* **1991**, *403*, 269−277. (f) Milani, B.; Alessio, E.; Mestroni, G.; Sommazzi, A.; Garbassi, F.; Zangrando, E.; Bresciani-Pahor, N.; Randaccio, L. *J. Chem. Soc., Dalton Trans.* **1994**, 1903−1911. (g) Cucciolito, M. E.; De Renzi, A.; Giordano, F.; Ruffo, F. *Organometallics* **1995**, *14*, 5410−5414.

(13) Specific values reported in the text for δ, $^1J_{PtP}$, and $^2J_{PtH}$ refer to **6**.

Table 3. Counteranion, Solvent, and Nucleophile Dependence of the Rates of Flipping of Dmphen, $k_{f(333)}$, and of Aryl Rotation around the P−C_{ipso} Bond, $k_{rot(333)}$, in the Cyclometalated Complexes [Pt(dmphen)((P(*o*-tolyl)$_2$-Ph−CH_2-*k C,P*))]X

complex	X	solvent	[Me_2S] mM	$k_{f(333)}$ (s^{-1})	$\Delta G_f^{\ddagger}{}_{333}$ (kJ mol^{-1})	$k_{rot(333)}$ (s^{-1})	$\Delta G_{rot}^{\ddagger}(_{333})$ (kJ mol^{-1})
6	PF_6	$C_2D_2Cl_4$		14.7	74.5 ± 0.2	32 700	53.1 ± 0.9
7	SbF_6	$C_2D_2Cl_4$				36 000	52.9 ± 0.1
8	CF_3SO_3	$C_2D_2Cl_4$		26.6	72.7 ± 0.1	9300	56.6 ± 0.5
9	BF_4	$C_2D_2Cl_4$				36 400	52.8 ± 0.6
10	BArf	$C_2D_2Cl_4$				15 700	55.2 ± 0.2
6	PF_6	$CDCl_3$		250		85[a]	
6	PF_6	acetone-d_6		310		95[a]	
6	PF_6	CD_3OD		350		93[a]	
6	PF_6	$C_2D_2Cl_4$	5	15[b]		190[c]	
6	PF_6	$C_2D_2Cl_4$	30	70[b]		190[c]	
6	PF_6	$C_2D_2Cl_4$	60	100[b]		190[c]	
6	PF_6	$C_2D_2Cl_4$	110	180[b]		190[c]	
6	PF_6	$C_2D_2Cl_4$	170	300[b]		190[c]	

[a] At 227.2 K. [b] At 305.0 K. [c] At 249.8 K.

1H); 7.94 (s,1H); 7.86 (s, 1H); 7.61 (br, 1H); 7.50 (br, 1H); 7.33 (br, 3H); 7.13 (s, 2H); 6.98 (br, 1H); 6.92 (br, 1H), which belong to the aryl rings of the phosphane and, (ii) in the aliphatic region, two broad signals of the methylenic protons of the $-CH_2-$ group of the cyclometalated Pt{$CH_2C_6H_4$P(*o*-tolyl)$_2$-*κ*C,P} ring (δ 4.14 (br, 1H, C$H_{2a'}$); 3.83 (br, 1H, CH_{2a})), (iii) two signals for the methyl protons of the phenanthroline ligand (δ 3.12, CH_{3A} and δ 1.95, CH_{3B}), (iv) a set of two different single signals for the methyl substituent groups in the ortho position to the aryl rings on the phosphorus atom indicating their inequivalence (δ 1.60, CH_{3X}; 2.31, CH_{3Y}). A dynamic ^{1}H NMR spectrum of **6** in tetrachloroethane-d_2 is shown in Figure 5.

Variable-temperature ^{1}H NMR spectra revealed the rapid coalescence of the signals of most of the aryl protons and of both methyl and methylenic protons of the Pt{$CH_2C_6H_4$P(*o*-tolyl)$_2$-*κ*C,P} ligand. Over 330 K, these two sets of signals become equivalent, giving a single peak at δ = 2.32 ppm and a multiplet at δ 3.77, $^2J_{PtH}$ = 100 Hz, respectively. These findings indicate that at low temperature the coordination plane does not act as a mirror plane and reveal a new phenomenon, that is, restricted rotation around the P−C_{ipso}(*o*-tolyl) bonds. Flapping the butterfly wings must also be at least as fast as rotation about the P−C bonds. The full line-shape analysis of the ortho methyl and of the methylenic protons resonances and fitting to the Eyring equation for **6** led to k_{333} = (32 700) s^{-1}, $\Delta H^{\ddagger}$ = (37.6 ± 2.1) kJ mol^{-1}, $\Delta S^{\ddagger}$ = (−46.6 ± 9) J K^{-1} mol^{-1}, and $\Delta G^{\ddagger}_{333}$ = (53.1 ± 0.9) kJ mol^{-1} for the rate and activation parameters of the P−C_{ipso}(*o*-tolyl) bond rotation process. Primary kinetic data and activation parameters for **6**−**10** are collected in Table SI3 in the Supporting Information.

At room temperature, the dmphen oscillation of **6** is still frozen. The loss of inequivalence of the two halves of the symmetric phenanthroline ligand starts up to 345 K. The full line-shape analysis of the rate data, obtained as described above, and fitting to the Eyring equation led to k_{333} = (14.7) s^{-1}, $\Delta H^{\ddagger}$ = (79.3 ± 1.4) kJ mol^{-1}, $\Delta S^{\ddagger}$ = (14.4 ± 4) J K^{-1} mol^{-1}, and $\Delta G^{\ddagger}_{333}$ = (74.5 ± 0.2) kJ mol^{-1} for the flipping of dmphen within cyclometalated **6**. The same analysis has been accomplished also for **8** but **7**, **9**, and **10** maintained a static pattern up to 400 K. Primary kinetic data and activation parameters for **6** and **8** are collected in Table SI4 in the Supporting Information. Variable-temperature ^{1}H NMR spectra of **6** were monitored as a function of the solvents and of the concentration of added nucleophiles. In Table 3 are collected rate constants and the associated activation parameters for the two independent ligand motions.

Discussion.

A Molecular Gear. The distortion of the ligand dmphen, that can be seen in the molecular structure of a variety of [Pt(Me)(dmphen)(L)]X[1−4] and similar compounds,[12] is the prevalent cause of the phenomenon of its oscillation, but a multiplicity of factors can play a concurrent role, such as the nature and the size of the coordinated ligand L, the coordinating properties of the counteranion, of the solvent, or of the deliberate addition of nucleophiles acting as catalysts. Factors favoring lengthening of the Pt−N bonds and dissociation are (i) the high trans influence of the strong *σ*-electron-donor methyl and phosphane groups, (ii) the additional steric congestion at the coordination plane brought about by the *cis*-phosphane. At the same time, the easy addition of a fifth group to the metal is favored by the fact that in a bipyramidal five-coordinated species the phenanthroline becomes planar again, occupying two sites of the equatorial plane and releasing a remarkable amount of steric strain.[14] Thus, the mechanism of flipping is switchable between intramolecular dissociative and bimolecular associative pathways, in a delicate equilibrium that is governed by the relative importance of the various parameters indicated

(14) (a) Albano, V. G.; Natile, G.; Panunzi, A. *Coord. Chem. Rev*. **1994**, *133*, 67−114. (b) Maresca, L.; Natile, G. *Comments Inorg. Chem.* **1993**, *14*, 349−366. (c) Romeo, R.; Monsù Scolaro, L.; Nastasi, N.; Arena, G. *Inorg. Chem.* **1996**, *35*, 5087−5096. (d) Albano, V. G.; Ferrara, M. L.; Monari, M.; Panunzi, A.; Ruffo, F. *Inorg. Chim. Acta* **1999**, *285*, 70−75. (e) De Felice, V.; Ferrara, M. L.; Giordano, F.; Ruffo, F. *Gazz. Chim. Ital.* **1994**, *124*, 117−119. (f) Giordano, F.; Ruffo, F.; Saporito, A.; Panunzi, A. *Inorg. Chim. Acta* **1997**, *264*, 231−237. (g) Fanizzi, F. P.; Natile, G.; Lanfranchi, M.; Tiripicchio, A.; Pacchioni, G. *Inorg. Chim. Acta* **1998**, *275*, 500−509. (h) Albano, V. G.; Castellari, C.; Monari, M.; De Felice, V.; Panunzi, A.; Ruffo, F. *Organometallics* **1996**, *15*, 4012−4019. (i) Albano, V. G.; Castellari, C.; Monari, M.; De Felice, V.; Panunzi, A.; Ruffo, F. *Organometallics* **1992**, *11*, 3665−3669. (j) Fanizzi, F. P.; Margiotta, N.; Lanfranchi, M.; Tiripicchio, A.; Pacchioni, G.; Natile, G. *Eur. J. Inorg. Chem.* **2004**, *8*, 1705−1713.

Scheme 2. Dissociative Mechanism Involving Three-Coordinated T-shaped Intermediates ($\mathbf{I_1}-\mathbf{I_4}$) for the Coupled Rotation-Flipping Motion

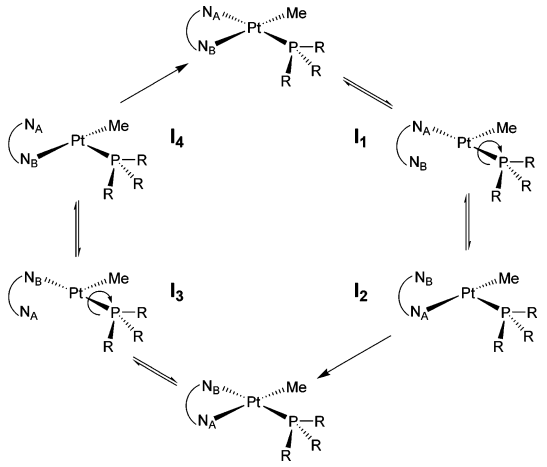

above. This mechanistic framework appears to be fully operative for a series of phosphorus-donor ligands of widely different stereoelectronic properties but is broken up when using ligands bearing bulky *o*-methoxyphenyl groups on the phosphorus donor atom such as P(2-$MeOC_6H_4)_3$, P(2-$MeOC_6H_4)_2$Ph, or P(2-$MeOC_6H_4$)Ph_2 phosphanes[4] or, in the present case, the P(2-$MeC_6H_4)_3$ phosphane. We showed before[4] that (i) the rates of flipping of dmphen and that of phosphane rotation around the Pt−P bond exhibited identical values, decreasing in a synchronous way with increasing steric congestion at PR_3, (ii) the rate of phosphane rotation was not influenced by the coordinative environment and particularly on whether the phenanthroline was flat or distorted, dynamic, or static in solution, (iii) the fluxional motion of dmphen was strongly affected by the size of PR_3 but was hardly sensitive to external stimuli (nature of the counterion, of the solvent, and deliberate addition of weak nucleophiles). In other words, the fluxional motion of dmphen was controlled by the slow rotation rate of the crowded phosphane and not vice versa. The circumstance that the [Pt(Me)(dmphen)(P(*o*-tolyl)$_3$)]X compounds behave exactly like the P(2-$MeOC_6H_4)_{3-n}Ph_n$ analogues rules out any conjecture about a decisive involvement of the oxygen atom of the methoxy group in the reaction intermediates depicted in Chart 1. Furthermore, the hypothesis of an intramolecular turnstile rearrangement in a five-coordinate intermediate (structure B in Chart 1) becomes a rather unlikely alternative to the dissociative mechanism in Scheme 2.

This latter involves (i) platinum−nitrogen bond breaking and formation of the two T-shaped three-coordinated intermediates $\mathbf{I_1}$ and $\mathbf{I_3}$ containing η^1-coordinated dmphen, (ii) their isomerization into the corresponding intermediates $\mathbf{I_2}$ and $\mathbf{I_4}$, and (iii) final ring closing. Formation of $\mathbf{I_1}$ through Pt−N bond breaking is not the rate-determining step for both motions. Rather, the most-energy spending pathways are (i) the mutual geometrical conversion of T-shaped three-coordinate [Pt(Me)(η^1-dmphen)(PR_3)]$^+$ intermediates (from $\mathbf{I_1}$ to $\mathbf{I_2}$) and, (ii) ring closing. Therefore, we conclude that steric congestion is at the origin of the connection of two otherwise independent motions, and oscillation of dmphen between the two nonequivalent exchanging sites must await for a 120° phosphane rotation around the platinum−phosphorus bond before being achieved. The lack of a catalytic effect by the addition of external nucleophiles is a further indication that the synchronized fluxional mechanism does not require the formation of a five-coordinated intermediate.

Cyclometalation Kinetics. Cyclometalation reactions represent examples of intramolecular C−H bond activation mediated by transition metals.[15] On increasing the temperature in $C_2H_2Cl_4$, **1**−**5** yielded the cyclometalated **6**−**10** by ortho metalation with the loss of methane, as shown in Scheme 1. The process within the cationic species is not affected by the nature of the counteranion ($CF_3SO_3^-$ for **3** vs BF_4^- for **4**, Figure 3). Among tertiary phosphines, P(*o*-tolyl)$_3$ appears to be particularly appropriate for cyclometalation reactions, because the value of the cone angle is fairly high (198°, from crystallographic measurements)[16] and the activation of one hydrogen of the CH_3 in the *o*-tolyl substituent leads to a particularly stable five-membered C−M−P ring. Examples of platinum derivatives containing the Pt{$CH_2C_6H_4$P(*o*-tolyl)$_2$-$\kappa C,P$} fragment can be found in the phosphane−platinum chemistry.[17a−f] Recently, we focused on the possibility of overcoming the kinetic inertness of 16-electron square-planar complexes toward C−H activation using electron-rich compounds, choosing among those complexes that have shown, in other reactions, particularly nucleophilic substitutions, a pronounced propensity to dissociate ligands vacating a coordination site.[18] Thus, we proved that dissociation of a ligand is a prerequisite for cyclometalation of *cis*-[Pt(Me)$_2$(dmso)(P(*o*-tolyl)$_3$)], leading to [Pt(Me)(dmso){$CH_2C_6H_4$P(*o*-tolyl)$_2$-$\kappa C,P$}] and methane,[19] and of the dinuclear Pt(II) compound of formula [Pt_2(μ-$SEt_2)_2$(Hbph)$_4$], (Hbph$^-$ = η^1-biphenyl monoanion), yielding [Pt_2(μ-$SEt_2)_2$(bph)$_2$] and biphenyl.[20] The coordinative and electronic unsaturation at the metal atom in the three-

(15) For recent reviews on cyclometallation, see (a) Crabtree, R. H. *J. Organomet. Chem.* **2005**, *690*, 5451−5457. (b) Slagt, M. Q.; van Zwieten, D. A. P.; Moerkerk, A. J. C. M.; Gebbink, R. J. M. K.; van Koten, G. *Coord. Chem. Rev.* **2004**, *248*, 2275−2282. (c) Omae, I. *Coord. Chem. Rev.* **2004**, *248*, 995−1023. (d) Werner, H. *Dalton Trans.* **2003**, *20*, 3829−3837. (d) Ryabov, A. D. *Chem. Rev.* **1990**, *90*, 403−424. (e) Newkome, G. R.; Puckett, W. E.; Gupta, V. K.; Kiefer, G. E. *Chem. Rev.* **1986**, *86*, 451−489.

(16) Ferguson, G.; Roberts, P. J.; Alyea, E. C.; Khan, M. *Inorg. Chem.* **1978**, *17*, 2965−2967.

(17) a) Casas, J. M.; Forniés, J.; Fuertes, S.; Martín, A.; Sicilia, V. *Organometallics* **2007**, *26*, 1674−1685 and references therein. (b) Ara, I.; Forniés, J.; Sicilia, V.; Villarroya, P. *Dalton Trans.* **2003**, 4238−4242. (c) Falvello, L. R.; Forniés, J.; Martín, A.; Sicilia, V.; Villarroya, P. *Organometallics* **2002**, *21*, 4604−4610. (d) Forniés, J.; Martín, A.; Navarro, R.; Sicilia, V.; Villarroya, P. *Organometallics* **1996**, *15*, 1826−1833. (e) Falvello, L. R.; Forniés, J.; Martín, A.; Navarro, R.; Sicilia, V.; Villarroya, P. *Inorg. Chem.* **1997**, *36*, 6166−6171. (f) Chappell, S. D.; Cole-Hamilton, D. J. *J. Chem. Soc., Dalton Trans.* **1983**, 1051−1057. (g) Cheney, A. J.; Shaw, B. L. *J. Chem. Soc., Dalton Trans.* **1972**, 754−763. (h) Thorn, D. L. *Organometallics* **1998**, *17*, 348−352. (i) Alyea, E. C.; Ferguson, G.; Malito, J.; Ruhl, B. L. *Organometallics* **1989**, *8*, 1188−1191. (j) Alyea, E. C.; Malito, J.; Ruhl, B. L. *J. Organomet. Chem.* **1988**, *340*, 119−126. (k) Scheffknecht, C.; Rhomberg, A.; Müller, E. P.; Peringer, P.; *J. Organomet. Chem.* **1993**, *463*, 245−248. (l) Clark, H. C.; Goel, A. B.; Goel, R. G.; Goel, S. *Inorg. Chem.* **1980**, *19*, 3220−3225.

(18) Refs 19 and 20 should be consulted for a discussion on the dissociative reaction pathways in Pt(II) chemistry, the generation and fate of three-coordinate intermediates, and for a list of references to previous work in the field.

(19) Romeo, R.; Plutino, M. R.; Romeo, A. *Helv. Chim. Acta* **2005**, *88* (3), 507−522.

Scheme 3. Oxidative Addition-Reductive Elimination Mechanism for Orthoplatination of **1**−**5**

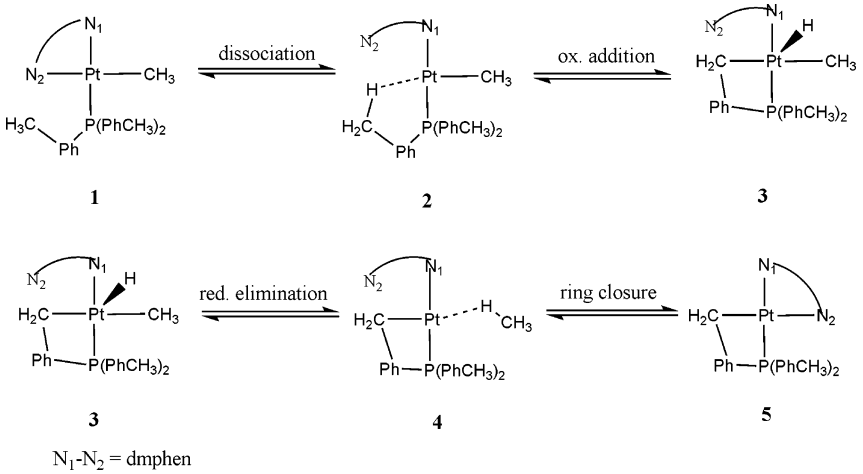

coordinate, 14-electron, T-shaped complex favors an initial agostic interaction involving an empty orbital on platinum and the electron pair of the C−H bond.[21] Oxidative addition of the C−H bond follows, yielding a cyclometalated-hydrido 16-electron Pt(IV) five-coordinate intermediate. Finally, reductive elimination with the elimination of alkane or arene yields the cyclometalated compounds. This multistep mechanism has been supported by subsequent DFT calculations.[22]

We are inclined to think that opening of the dmphen ring and formation of a T-shaped unsaturated three-coordinated species is a preliminary step in the orthoplatination of [Pt(Me)(dmphen)(P(*o*-tolyl)$_3$)]X, **1**−**5**, leading to [Pt(dmphen)-{$CH_2C_6H_4P$(*o*-tolyl)$_2$-$\kappa C,P$}]X cyclometalated Pt(II) compounds **6**−**10**. Cyclometalation on **1**−**5** develops along the key steps in Scheme 3, namely (i) reversible dmphen ring opening and closing, (ii) oxidative addition of the C−H bond to the unsaturated T-shaped intermediate containing η^1-coordinated dmphen, (iii) reductive elimination from a Pt(IV) hydride species, with liberation of methane, and (iv) final dmphen ring closure.

The oxidative addition-reductive elimination mechanism in Scheme 3 is substantiated by (i) the ease with which a Pt−N bond can be broken in **1** to yield [Pt(Me)(η^1-dmphen)-(P(*o*-tolyl)$_3$)] (the corresponding unhindered [Pt(Me)(phen)-(P(*o*-tolyl)$_3$)] complex does not exhibit either phenanthroline flipping or orthoplatination), and (ii) the growing wealth of evidence for the operation of an oxidative-addition mechanism not only in intramolecular but also in intermolecular processes of C−H bond activation by Pt(II) compounds. The interpretation of the activation parameters ($\Delta H^{\ddagger} = 59.3 \pm 3$ kJ mol^{-1}, $\Delta S^{\ddagger} = -141 \pm 8$ J K^{-1} mol^{-1}) is not straightforward because, at this stage, they cannot be assigned to a single step, but the largely negative value of the entropy of activation could be indicative a more-compact transition state (five-coordinate) rather than an open transition state (three-coordinate) with respect to the starting four-coordinate, 16-electron complex. Thus, the overall kinetic analysis of the system supports the involvement of a five-coordinate Pt(IV), two three-coordinate Pt(II) species, and a Pt(II) C−H σ-methane complex as reaction intermediates. The principle of microscopic reversibility requires also preliminary ring opening of dmphen at square-planar Pt(II) **5** prior to methane oxidative addition, a fundamental step in the Shilov alkane oxidation system.[23] The hydrido platinum(IV) intermediate should have a square-planar pyramidal geometry, as indicated by several theoretical studies[24] and by a recent isolation and structural characterization of some of such compounds.[25] Hydridoplatinum(IV) intermediates have been proposed in the synthesis of cyclometalated complexes containing bidentate (C,N) or terdentate (C,N,N′) ligands,[26] in the thermolysis of different platinum dialkyl complexes that lack β-H-atoms, leading to the formation of metallacycles along with the corresponding hydrocarbons,[27] in the intermolecular C−H activation of alkanes and arenes accomplished under mild conditions by complexes of the form [Pt(N−N)(Me)-

(20) Plutino, M. R.; Monsù Scolaro, L.; Albinati, A.; Romeo, R. *J. Am. Chem. Soc.* **2004**, *126*, 6470−6484.
(21) Romeo, R.; D'Amico, G.; Sicilia, E.; Russo, N.; Rizzato, S. *J. Am. Chem. Soc.* **2007**, *129*, 5744−5755.
(22) Romeo, R. et al.; unpublished results.
(23) Shilov, A. E.; Shul'pin, G. B. *Chem. Rev.* **1997**, *97*, 2879−2932.
(24) (a) Hill, G. S.; Puddephatt, R. J. *Organometallics* **1998**, *17*, 1478−1486. (b) Siegbahn, P. E. M.; Crabtree, R. H. *J. Am. Chem. Soc.* **1996**, *118*, 4442−4450. (c) Bartlett, K. L.; Goldberg, K. I.; Borden, W. T. *J. Am. Chem. Soc.* **2000**, *122*, 1456−1465. (d) Bartlett, K. L.; Goldberg, K. I.; Borden, W. T. *Organometallics.* **2001**, *20*, 2669−2678. (e) Heiberg, H.; Johansson, L.; Gropen, O.; Ryan, O. B.; Swang, O.; Tilset, M. *J. Am. Chem. Soc.* **2000**, *122*, 10831−10845. (f) Gilbert, T. M.; Hristov, I.; Ziegler, T. *Organometallics* **2001**, *20*, 1183−1189.
(25) (a) Fekl, U.; Kaminsky, W.; Goldberg, K. I. *J. Am. Chem. Soc.* **2001**, *123*, 6423−6424. (b) Reinartz, S.; White, P. S.; Brookhart, M.; Templeton, J. L. *J. Am. Chem. Soc.* **2001**, *123*, 12724−12725.
(26) (a) Anderson, C. M.; Crespo, M. *J. Organomet. Chem.* **2004**, *689*, 1496−1502. (b) Anderson, C. M.; Crespo, M.; Font-Bardia, M.; Klein, A.; Solans, X. *J. Organomet. Chem.* **2000**, *601*, 22−33. (c) van Der Boom, M. E.; Ott, J.; Milstein, D. *Organometallics* **1999**, *18*, 3873−3884. (d) Crespo, M.; Solans, X.; Font-Bardia, M. *Organometallics* **1995**, *14*, 355−364. (e) Anderson, C. M.; Crespo, M.; Jennings, M. C.; Lough, A. J.; Ferguson, G.; Puddephatt, R. J. *Organometallics* **1991**, *10*, 2672−2679.
(27) (a) Foley, P.; Whitesides, G. M. *J. Am. Chem. Soc.* **1979**, *101*, 2732−2733. (b) Foley, P.; Di Cosimo, R.; Whitesides, G. M. *J. Am. Chem. Soc.* **1980**, *102*, 6713−6725. (c) Moore, S. S.; Di Cosimo, R.; Sowinski, A. F.; Whitesides, G. M. *J. Am. Chem. Soc* **1981**, *103*, 948−949. (d) Di Cosimo, R.; Moore, S. S.; Sowinski, A. F.; Whitesides, G. M. *J. Am. Chem. Soc.* **1982**, *104*, 124−133. (e) Chappell, S. D.; Cole-Hamilton, D. J. *J. Chem. Soc., Chem. Commun.* **1980**, 238−239. (f) Chappell, S. D.; Cole-Hamilton, D. J. *J. Chem. Soc., Dalton Trans.* **1983**, 1051−1057. (g) Griffiths, D. C.; Young, G. B. *Polyhedron* **1983**, *2*, 1095−1100. (h) Hackett, M.; Ibers, J. A.; Whitesides, G. M. *J. Am. Chem. Soc* **1988**, *110*, 1436−1448. (i) Griffiths, D. C.; Young, G. B. *Organometallics* **1989**, *8*, 875−886.

(solv)]$^+$ (N−N is a bidentate nitrogen-centered ligand and solv is a weakly coordinating solvent).[28]

In conclusion, as in the cases studied previously,[19,20] the cycloplatination process of **1**−**5** follows a dissociative pathway, but dissociation does not seem to be the rate-determining step. A ring-opening ring-closing pre-equilibrium is established that controls the concentration of unsaturated three-coordinate T-shaped intermediates. A multistep mechanism of oxidative addition/reductive elimination follows, and, at this stage, a DFT study could help in assessing with confidence which of these two steps is rate limiting.

Structural and Dynamic Characteristics of Cyclometalated Complexes. The cationic complex [Pt{$CH_2C_6H_4P$-(*o*-tolyl)$_2$-$\kappa C,P$}(dmphen)] shows a butterfly shape with asymmetric wings due to the distortion away of the two rings from the square coordination plane (Figure 4). Steric congestion is still large enough to promote a slow oscillation of the symmetric chelating ligand dmphen. This fluxional motion is markedly sensitive to the nature of the counteranion X and of the solvent (rates and activation data in Table 3). The flipping rate can be significantly accelerated by the deliberate addition of external weak nucleophiles (Me_2S). A plot of k_f against the nucleophile concentration is linear with a definite, even though it is small, intercept (Figure SI1 in the Supporting Information). Thus, the oscilla

$$k_f = k_1 + k_2\,[Me_2S] \qquad (1)$$

tion of the nitrogen ligand obeys the two-term rate law, which is identical to the well-known rate that controls nucleophilic substitution reactions on square-planar complexes. Here, k_1 (7 ± 8 s^{-1} in $C_2D_2Cl_4$ at 305.0 K for **6**) represents the rate of uncatalyzed dmphen flipping, and k_2 (1.7 ± 0.09 mM^{-1} s^{-1}) gives a measure of the catalytic efficiency of Me_2S. This catalytic effect was explained previously[2] with the operation of a bimolecular stepwise displacement mechanism, so that the catalytic efficiency, as the nucleophilic ability, depends upon the stereoelectronic characteristics of the catalysts. Thus, cyclometalation leads to a changeover of the flipping mechanism, from dissociative in **1**−**5** to associative in **6**−**10**, confirming the delicate tuning of activation modes brought about by small structural changes. The use of catalysts can help to overcome the fluxional inertness of **7**, **9**, and **10**, possibly due to the formation of tight ion pairs.

Dynamic ^{1}H NMR spectra revealed a new fluxional motion given by restricted rotation of the *o*-tolyl rings around the P−C_{ipso} bonds. The free activation energy calculated from full line-shape analysis was $\Delta G^{\ddagger}_{333} = (53.1 \pm 0.9)$ kJ mol^{-1} and compares well with the value $\Delta G^{\ddagger}_{318} = (66.5)$ kJ mol^{-1} calculated from the coalescence temperature for the cyclometalated analog [Pt($CH_2C_6H_4P$(*o*-tolyl)$_2$-$\kappa C,P$}(S_2CNMe_2)].[17d] Line-shape analysis of the proton ortho methyl resonances gave a value of $\Delta G^{\ddagger}_{238}$ of 50.2 kJ mol^{-1} for the ring exchange in [Cr(C_6H_6)(CO)$_2$(*o*-tolyl)$_3$],[29] considerably higher than analogous processes in [Cr(CO)$_5$(P(*o*-tolyl)$_3$)] and [Fe(CO)$_4$-(P(*o*-tolyl)$_3$)] ($\Delta G^{\ddagger}_{233}$ = 38.6 and 44.6 kJ mol^{-1}, respectively).[30] Interestingly, the highest energy barrier for ring rotation seems to fit in the *cis*-[Pt(Me)$_2$(dmso)(P(*o*-tolyl)$_3$)] complex that, because of the very low rate of ring exchange, exists in two differently populated conformations in solution at remarkably high temperatures.[19] For rotation of a phenyl group of the unhindered PPh_3, an upper limit of $\Delta G^{\ddagger}_{218}$ = 30 kJ mol^{-1} has been observed in complexes of the type *cis*-[PtX_2(dmphen)(PPh_3)] and *trans*-[PtX (dmphen)(PPh_3)$_2$] (X = Cl, Br, I), as a result of stacking interactions that behave as a brake, contributing significantly to the increase of the usually very low energy barrier of this process.[31]

Experimental Section

General Procedures and Chemicals. Microanalyses were performed by the Microanalytical Laboratory: University of Dublin, Ireland. ^{1}H NMR and ^{31}P NMR spectra were recorded using a Bruker AMX-300 spectrometer. The ^{1}H resonance of the solvent was used as an internal standard, but chemical shifts are reported with respect to Me_4Si. ^{31}P{^{1}H} NMR shifts are referenced to external 85% H_3PO_4. The data are reported as follows: chemical shift in ppm (δ) units, multiplicity, coupling constants (Hz), and integration. The temperature within the probe was checked using the methanol method.[32] All of the preparations and other operations were carried out under oxygen-free nitrogen following conventional Schlenk techniques. Solvents employed in the synthetic procedures (Analytical Reagent Grade, Lab-Scan Ltd.) were distilled under nitrogen from sodium-benzophenone ketyl (tetrahydrofuran, diethyl ether, toluene) or barium oxide (dichloromethane). The petroleum ether used had a boiling point of 40−60 °C. Chloroform-*d* (D, 99.96%, Cambridge Isotope Laboratories) was dried standing for many days over CaH_2, distilled under nitrogen over activated magnesium sulfate and sodium carbonate, and then stored over activated 4 Å molecular sieves. Acetone-d_6, CD_3OD, and 1,1,2,2-tetrachloroethane-d_2 were used as received from CIL. The silver salts, 2,9-dimethyl-1,10-phenanthroline, and 3-*o*-tolylphosphane were purchased from Aldrich Chemical Co. The salt Na[B(3,5-$(CF_3)_2C_6H_3)_4$] was prepared according to a published method.[33]

(28) (a) Williams, T. J.; Labinger, J. A.; Bercaw, J. E. *Organometallics*, **2007**, *26*, 281−287. (b) Driver, T. G.; Williams, T. J.; Labinger, J. A.; Bercaw, J. E. *Organometallics*, **2007**, *26*, 294−301. (c) Lersch, M.; Tilset, M. *Chem. Rev.* **2005**, *105*, 2471−2526. (d) Labinger, J. A.; Bercaw, J. E. *Nature* **2002**, *417*, 507−514. (e) Zhong, H. A.; Labinger, J. A.; Bercaw, J. E. *J. Am. Chem. Soc.* **2002**, *124*, 1378−1399. (f) Johansson, L.; Tilset, M.; Labinger, J. A.; Bercaw, J. E. *J. Am. Chem. Soc.* **2000**, *122*, 10846−10855. (g) Procelewska, J.; Zahl, A.; van Eldik, R.; Zhong, H. A.; Labinger, J. A.; Bercaw, J. E. *Inorg. Chem.* **2002**, *41*, 2808−2810. (h) Johansson, L.; Ryan, O. B.; Tilset, M. *J. Am. Chem. Soc.* **1999**, *121*, 1974−1975. (i) Johansson, L.; Ryan, O. B.; Römming, C.; Tilset, M. *J. Am. Chem. Soc.* **2001**, *123*, 6579−6590. (j) Johansson, L.; Tilset, M. *J. Am. Chem. Soc.* **2001**, *123*, 739−740. (k) Holtcamp, M. W.; Henling, L. M.; Day, M. W.; Labinger, J. A.; Bercaw, J. E. *Inorg. Chim. Acta* **1998**, *270*, 467−478. (l) Periana, R. A.; Taube, D. J.; Gamble, S.; Taube, H.; Satoh, T.; Fujii, H. *Science* **1998**, *280*, 560−564. (m) Wick, D. D.; Goldberg, K. I. *J. Am. Chem. Soc.* **1997**, *119*, 10235−10236. (n) Fekl, U.; Goldberg, K. I. *Adv. Inorg. Chem.* **2003**, *54*, 259−320.

(29) Howell, J. A. S.; Palin, M. G.; McArdle, P.; Cunningham, D.; Goldschmidt, Z.; Gottlieb, H. E.; Hezroni-Langerman, D. *Organometallics* **1993**, *12*, 1694−1701.

(30) Howell, J. A. S.; Palin, M. G.; McArdle, P.; Cunningham, D.; Goldschmidt, Z.; Gottlieb, H. E.; Hezroni-Langerman, D. *Inorg. Chem.* **1991**, *30*, 4683−4685.

(31) Fanizzi, F. P.; Lanfranchi, M.; Natile, G.; Tiripicchio, A. *Inorg. Chem.* **1994**, *33*, 3331−3339.

(32) (a) Van Geet, A. L. *Anal. Chem.* **1968**, *40*, 2227−2229. (b) Van Geet, A. L. *Anal. Chem.* **1970**, *42*, 679−680.

Synthesis of Complexes. The compounds *cis*-[$PtCl_2(Me_2SO)_2$][34] and *trans*-[$Pt(Me)Cl(Me_2SO)_2$][35] were synthesized by following earlier reported procedures.

[Pt(Me)Cl(dmphen)]. Upon adding a weighted amount of dmphen (237.0 mg, 1.08 mmol) in methanol (10 mL) to a solution of *trans*-[$Pt(Me)Cl(Me_2SO)_2$] (441.2 mg, 1.08 mmol) in methanol (30 mL), a bright-yellow precipitate immediately formed, which was filtered off, washed with methanol to eliminate traces of dimethylsulfoxide, and air-dried (88.5% yield). Anal. Calcd for $C_{15}H_{15}ClN_2Pt$: C,39.70; H, 3.33; N, 6.17. Found: C,40.11; H, 3.23; N, 6.37. ^{1}H NMR ($CDCl_3$, T = 298 K): δ 8.31 (d, 1H, H_4); 8.28 (d, 1H, H_7); 7.76 (s, 2H, $H_{5,6}$); 7.60 (d, 1H, H_3); 7.54 (d, 1H, H_8); 2.95 (s, 3H, CH_{3A}); 1.70 (s, 3H, CH_{3B}); 1.32 (s, $^2J_{Pt-H}$ = 80.3 Hz, 3H, Pt−CH_3).

[Pt(Me)(dmphen)(P(*o*-tolyl)$_3$)]X. (X = PF_6^-, **1**; SbF_6^-, **2**; $CF_3SO_3^-$, **3**; BF_4^-, **4**; BArf $^-$, **5**). The typical procedure was as follows. A known amount of [Pt(Me)Cl(dmphen)] in CH_2Cl_2 (15 mL) containing a few drops of methanol was dissolved by adding slowly under stirring a solution of the stoichiometric amount of AgX in acetone ($AgPF_6$, for **1**; $AgSbF_6$, for **2**; $AgCF_3SO_3$ for **3**; $AgBF_4$, for **4**). AgCl was separated out, the solution was filtered on a cellulose column to remove residual AgCl, and added with the stoichiometric amount of three-*o*-tolylphosphane upon cooling under dinitrogen atmosphere. The reaction was left to go to completion (within a couple of hours), the excess solvent was evaporated under reduced pressure, and the residue was crystallized in good yield from dichloromethane/diethyl ether. The synthesis of **5** required the use of NaBArf in dichloromethane instead of a silver salt and the elimination of solid NaCl.

[Pt(Me)(dmphen)(P(*o*-tolyl)$_3$)]PF_6 (1). (87.2% yield) Anal. Calcd for $C_{36}H_{36}F_6N_2P_2Pt$: C, 49.83; H, 4.18; N, 3.23. Found: C, 49.68; H, 4.22; N, 2.97. ^{1}H NMR ($CDCl_3$, T = 298 K): δ 8.55 (d, 1H, H_4); 8.40 (d, 1H, H_7); 8.00 (s, 2H, $H_{5,6}$); 7.76 (d, 1H, H_3); 7.01−7.43 (m, 13H, *H*-$P_{(Ar),}$ H_8); 3.58 (s, 3H, CH_{3z}); 2.95 (s, 3H, CH_{3A}); 1.78 (s, 3H, CH_{3B}); 1.50 (s, 3H, CH_{3y}); 0.85 (s, 3H, CH_{3x}); 0.59 (m, $^2J_{PtH}$ = 68 Hz, 3H, Pt−CH_3). ^{31}P NMR ($CDCl_3$, T = 298 K): δ 5.20 ($^1J_{PtP}$ = 4514 Hz).

[Pt(Me)(dmphen)(P(*o*-tolyl)$_3$)]SbF_6 (2). (67.3% yield). Anal. Calcd for $C_{36}H_{36}F_6N_2PPtSb$: C, 45.11; H, 3.79; N, 2.92. Found: C, 46.00; H, 3.90; N, 2.64. ^{1}H NMR ($CDCl_3$, T = 298 K): δ 8.54 (d, 1H, H_4); 8.39 (d, 1H, H_7); 7.96 (s, 2H, $H_{5,6}$); 7.85 (d, 1H, H_3); 7.01−7.67 (m, 12H, *H*-$P_{(Ar),}$); 6.87 (d, 1H, H_8); 3.58 (s, 3H, CH_{3z}); 2.95 (s, 3H, CH_{3A}); 1.78 (s, 3H, CH_{3B}); 1.50 (s, 3H, CH_{3y}); 0.85 (s, 3H, CH_{3x}); 0.60 (m, $^2J_{Pt-H}$ = 69 Hz, 3H, Pt−CH_3). ^{31}P NMR ($CDCl_3$, T = 298 K): δ 5.20 ($^1J_{PtP}$ = 4507 Hz).

[Pt(Me)(dmphen)(P(*o*-tolyl)$_3$)]CF_3SO_3 (3). (78.1% yield). Anal. Calcd for $C_{37}H_{36}F_3N_2O_3PPtS$: C, 50.97; H, 4.16; N, 3.21. Found: C, 49.42; H, 4.10; N, 2.99. ^{1}H NMR ($CDCl_3$, T = 298 K): δ 8.67 (d, 1H, H_4); 8.55 (d, 1H, H_7); 8.40 (s, 2H, $H_{5,6}$); 7.80 (d, 1H, H_3); 7.00−7.60 (m, 13H, *H*-$P_{(Ar)}$, H_8); 3.59 (s, 3H, CH_{3z}); 2.95 (s, 3H, CH_{3A}); 1.82 (s, 3H, CH_{3B}); 1.50 (s, 3H, CH_{3y}); 0.85 (s, 3H, CH_{3x}); 0.60 (m, $^2J_{PtH}$ = 71 Hz, 3H, Pt−CH_3). ^{31}P NMR ($CDCl_3$, T = 298 K): δ 5.21 ($^1J_{PtP}$ = 4507 Hz).

[Pt(Me)(dmphen)(P(*o*-tolyl)$_3$)]BF_4 (4). (88.2% yield). Anal. Calcd for $C_{36}H_{36}BF_4N_2PPt$: C, 53.41; H, 4.48; N, 3.46. Found: C, 53.20; H, 4.35; N, 3.40. ^{1}H NMR ($CDCl_3$, T = 298 K): δ 8.70 (d, 1H, H_4); 8.50 (d, 1H, H_7); 8.00 (s, 2H, $H_{5,6}$); 7.90 (d, 1H, H_3); 7.12−7.56 (m, 13H, *H*-$P_{(Ar),}$ H_8); 3.59 (s, 3H, CH_{3z}); 2.95 (s, 3H, CH_{3A}); 1.78 (s, 3H, CH_{3B}); 1.55 (s, 3H, CH_{3y}); 0.88 (s, 3H, CH_{3x}); 0.56 (m, $^2J_{Pt-H}$ = 74 Hz, 3H, Pt−CH_3). ^{31}P NMR ($CDCl_3$, T = 298 K): δ 5.23 ($^1J_{Pt-P}$ = 4502 Hz).

[Pt(Me)(dmphen)(P(*o*-tolyl)$_3$)]BArf (5). (63.3% yield). Anal. Calcd for $C_{68}H_{48}BF_{24}N_2PPt$: C, 51.50; H, 3.05; N, 1.77. Found: C, 53.01; H, 3.35; N, 1.58. ^{1}H NMR ($CDCl_3$, T = 298 K): δ 8.32 (d, 1H, H_4); 8.22 (d, 1H, H_7); 7.00−8.00 (m, 28H, *H*-$P_{(Ar),}$, $H_{5,6}$, H_8, H_3, *H*-BArf); 3.58 (s, 3H, CH_{3z}); 2.91 (s, 3H, CH_{3A}); 1.70 (s, 3H, CH_{3B}); 1.52 (s, 3H, CH_{3y}); 0.86 (s, 3H, CH_{3x}); 0.61 (m, $^2J_{PtH}$ = 69 Hz, 3H, Pt−CH_3). ^{31}P NMR ($CDCl_3$, T = 298 K): δ 5.13 ($^1J_{Pt-P}$ = 4514 Hz).

Cyclometalated [Pt(dmphen)(P(*o*-tolyl)$_2$-Ph−CH_2-κ*C,P*)]X (X = PF_6^-, (6); SbF_6^-, (7); $CF_3SO_3^-$, (8); BF_4^-, (9); BArf $^-$, (10)). In a typical procedure, a solution of **1**−**5** in tetrachloroethane was warmed at 360 K for a few hours in a sealed vial. The excess solvent was evaporated under reduced pressure, the residue was dissolved in dichloromethane, and the products were separated out on adding diethyl ether and cooling.

[Pt(dmphen)(P(*o*-tolyl)$_2$-Ph−CH_2-κ*C,P*)]PF_6 (6). (81.2% yield). Anal. Calcd for $C_{35}H_{32}F_6N_2P_2Pt$: C, 49.36; H, 3.79; N, 3.29. Found: C, 47.96; H, 3.63; N, 2.99. ^{1}H NMR ($C_2D_2Cl_4$, T = 233 K): δ 9.65 (br, 1H, *H*-$P_{(Ar)}$); 8.52 (d, $^3J_{HH}$ = 8.8 Hz, 1H, H_4); 8.30 (d, $^3J_{HH}$ = 8.8 Hz, 1H, H_7); 7.94 (s, 1H, *H*-$P_{(Ar)}$); 7.90 (d, $^3J_{HH}$ = 8.8 Hz, 2H, $H_{5,6}$); 7.86 (s, 1H, *H*-$P_{(Ar)}$); 7.61 (br, 1H, *H*-$P_{(Ar)}$); 7.50 (br, 1H, *H*-$P_{(Ar)}$); 7.33 (br, 3H, *H*-$P_{(Ar)}$); 7.19 (d, $^3J_{HH}$ = 8.8 Hz, 1H, H_3); 7.13 (s, 2H, *H*-$P_{(Ar)}$); 7.06 (d, $^3J_{HH}$ = 8.8 Hz, 1H, H_8); 6.98 (br, 1H, *H*-$P_{(Ar)}$); 6.92 (br, 1H, *H*-$P_{(Ar)}$); 4.14 (br, 1H, C$H_{2a'}$); 3.83 (br, 1H, CH_{2a}); 3.12 (s, 3H, CH_{3A}); 2.31 (br, 3H, CH_{3y}); 1.95 (s, 3H, CH_{3B}); 1.60 (br, 3H, CH_{3x}). ^{31}P NMR ($C_2D_2Cl_4$, T = 233 K): δ 30.3 ($^1J_{PtPav}$ = 4413 Hz).

[Pt(dmphen)(P(*o*-tolyl)$_2$-Ph−CH_2-κ*C,P*)]SbF_6 (7). (85.4% yield). Anal. Calcd for $C_{35}H_{32}F_6N_2PPtSb$: C, 44.60; H, 3.42; N, 2.97. Found: C, 44.82; H, 3.63; N, 2.98. ^{1}H NMR ($C_2D_2Cl_4$, T = 233 K): δ 9.65 (br, 1H, *H*-$P_{(Ar)}$); 8.52 (d, $^3J_{HH}$ = 8.8 Hz, 1H, H_4); 8.31 (d, $^3J_{HH}$ = 8.8 Hz, 1H, H_7); 7.94 (s, 1H, *H*-$P_{(Ar)}$); 7.90 (d, $^3J_{HH}$ = 8.8 Hz, 2H, $H_{5,6}$); 7.87 (s, 1H, *H*-$P_{(Ar)}$); 7.61 (br, 1H, *H*-$P_{(Ar)}$); 7.50 (br, 1H, *H*-$P_{(Ar)}$); 7.33 (br, 3H, *H*-$P_{(Ar)}$); 7.20 (d, $^3J_{HH}$ = 8.8 Hz, 1H, H_3); 7.14 (s, 2H, *H*-$P_{(Ar)}$); 7.06 (d, $^3J_{HH}$ = 8.8 Hz, 1H, H_8); 6.99 (br, 1H, *H*-$P_{(Ar)}$); 6.91 (br, 1H, *H*-$P_{(Ar)}$); 4.15 (br, 1H, C$H_{2a'}$); 3.83 (br, 1H, CH_{2a}); 3.13 (s, 3H, CH_{3A}); 2.31 (br, 3H, CH_{3y}); 1.95 (s, 3H, CH_{3B}); 1.60 (br, 3H, CH_{3x}). ^{31}P NMR ($C_2D_2Cl_4$, T = 233 K): δ 30.3 ($^1J_{PtPav}$ = 4413 Hz).

[Pt(dmphen)(P(*o*-tolyl)$_2$-Ph−CH_2-κ*C,P*)]CF_3SO_3 (8). (91.2% yield). Anal. Calcd for $C_{36}H_{32}F_3N_2O_3PPtS$: C, 50.53; H, 3.77; N, 3.27. Found: C, 49.20; H, 3.63; N, 3.12 ^{1}H NMR ($C_2D_2Cl_4$, T = 233 K): δ 9.64 (br, 1H, *H*-$P_{(Ar)}$); 8.52 (d, $^3J_{HH}$ = 8.8 Hz, 1H, H_4); 8.30 (d, $^3J_{HH}$ = 8.8 Hz, 1H, H_7); 7.93 (s, 1H, *H*-$P_{(Ar)}$); 7.89 (d, $^3J_{HH}$ = 8.8 Hz, 2H, $H_{5,6}$); 7.85 (s, 1H, *H*-$P_{(Ar)}$); 7.61 (br, 1H, *H*-$P_{(Ar)}$); 7.49 (br, 1H, *H*-$P_{(Ar)}$); 7.32 (br, 3H, *H*-$P_{(Ar)}$); 7.19 (d, $^3J_{HH}$ = 8.8 Hz, 1H, H_3); 7.13 (s, 2H, *H*-$P_{(Ar)}$); 7.05 (d, $^3J_{HH}$ = 8.8 Hz, 1H, H_8); 6.98 (br, 1H, *H*-$P_{(Ar)}$); 6.91 (br, 1H, *H*-$P_{(Ar)}$); 4.14 (br, 1H, C$H_{2a'}$); 3.83 (br, 1H, CH_{2a}); 3.11 (s, 3H, CH_{3A}); 2.30 (br, 3H, CH_{3y}); 1.94 (s, 3H, CH_{3B}); 1.59 (br, 3H, CH_{3x}). ^{31}P NMR ($C_2D_2Cl_4$, T = 233 K): δ 30.3 ($^1J_{PtPav}$ = 4413 Hz).

[Pt(dmphen)(P(*o*-tolyl)$_2$-Ph−CH_2-κ*C,P*)]BF_4 (9). (78.2% yield). Anal. Calcd for $C_{35}H_{32}BF_4N_2PPt$: C, 52.98; H, 4.06; N, 3.53. Found: C, 53.12; H, 3.93; N, 3.42 ^{1}H NMR ($C_2D_2Cl_4$, T = 233 K): δ 9.63 (br, 1H, *H*-$P_{(Ar)}$); 8.52 (d, $^3J_{HH}$ = 8.8 Hz, 1H, H_4); 8.30 (d, $^3J_{HH}$ = 8.8 Hz, 1H, H_7); 7.93 (s, 1H, *H*-$P_{(Ar)}$); 7.90 (d, $^3J_{HH}$ = 8.8 Hz, 2H, $H_{5,6}$); 7.86 (s, 1H, *H*-$P_{(Ar)}$); 7.59 (br, 1H, *H*-$P_{(Ar)}$); 7.48 (br, 1H, *H*-$P_{(Ar)}$); 7.31 (br, 3H, *H*-$P_{(Ar)}$); 7.17 (d, $^3J_{HH}$ = 8.8 Hz, 1H, H_3); 7.12 (s, 2H, *H*-$P_{(Ar)}$); 7.04 (d, $^3J_{HH}$ = 8.8 Hz, 1H, H_8);

(33) Brookhart, M.; Grant, B.; Volpe, A. F. *Organometallics* **1992**, *11*, 3920−3922.
(34) Price, J. H.; Williamson, A. N.; Schramm, R. F.; Wayland, B. B. *Inorg. Chem.* **1972**, *11*, 1280−1284.
(35) Eaborn, C.; Kundu, K.; Pidcock, A. *J. Chem. Soc., Dalton Trans.* **1981**, 933−938.

Table 4. Crystal Data and Structure Refinement Details for **10**[a]

empirical formula	$C_{134}H_{88}B_2F_{48}N_4P_2Pt_2$	
fw	3139.82	
T	150(2) (K)	
wavelength	0.71073 Å	
cryst syst	triclinic	
space group	$P\bar{1}$	
unit cell dimensions	$a = 13.189(1)$ Å	$\alpha = 84.902(3)°$
	$b = 18.421(2)$ Å	$\beta = 84.139(3)°$
	$c = 25.996(3)$ Å	$\gamma = 87.121(3)$
V	6253(1) Å^3	
Z	4	
d_{calcd}	1.668 Mg/m^3	
absorption coefficient	2.386 mm^{-1}	
F(000)	2756	
cryst size	0.2 × 0.2 × 0.02 mm^3	
θ range for data collection	1.42 to 27.02°	
index ranges	±16, ±23, ±33	
reflns collected	62757	
independent reflns	20402 [R(int) = 0.0399]	
completeness to $\theta = 27.02°$	99.2%	
refinement method	full-matrix least-squares on F^2	
data/restraints/params	27162/1409	
GOF on F^2	1.025	
Final R indices [$I > 2\sigma(I)$]	R1 = 0.0459, wR2 = 0.1050	
R indices (all data)	R1 = 0.0695, wR2 = 0.1149	
largest diff. peak and hole	1.893 and −0.891 e·Å^{-3}	

[a] $R_{int} = \sum|F_o^2 - \langle F_o^2\rangle|/\sum|F_o^2|$; $R = \sum(|F_o - (1/k)F_c|)/\sum|F_o|$; $R^2_w = \{\sum[w(F_o^2 - (1/k)F_c^2)^2]/\sum w|F_o^2|^2]\}^{1/2}$; GOF = $[\sum_w(F_o^2 - (1/k)F_c^2)^2/(n_o - n_v)]^{1/2}$.

6.97 (br, 1H, *H*-P$_{(Ar)}$); 6.90 (br, 1H, *H*-P$_{(Ar)}$); 4.14 (br, 1H, C*H*$_{2a'}$); 3.81 (br, 1H, C*H*$_{2a}$); 3.11 (s, 3H, C*H*$_{3A}$); 2.29 (br, 3H, C*H*$_{3y}$); 1.94 (s, 3H, C*H*$_{3B}$); 1.58 (br, 3H, C*H*$_{3x}$). ^{31}P NMR ($C_2D_2Cl_4$, $T = 233$ K): δ 30.3 ($^1J_{PtPav} = 4413$ Hz).

[Pt(dmphen)(P(*o*-tolyl)$_2$-Ph−CH$_2$-*κC,P*)]BArf(10). (98.6% yield). Anal. Calcd for $C_{67}H_{44}BF_{24}N_2PPt$: C, 51.26; H, 2.82; N, 1.78. Found: C, 49.80; H, 2.73; N, 1.65. ^{1}H NMR ($C_2D_2Cl_4$, $T = 233$ K): δ 9.66 (br, 1H, *H*-P$_{(Ar)}$); 8.38 (d, $^3J_{HH} = 8.8$ Hz, 1H, *H*$_4$); 8.17 (d, $^3J_{HH} = 8.8$ Hz, 1H, *H*$_7$); 7.74 (br, 12H, *H*-P$_{(Ar)}$, *H*$_{5,6}$, *H*-BArf); 7.50 (br, 6H, *H*-P$_{(Ar)}$, *H*-BArf); 7.31 (br, 3H, *H*-P$_{(Ar)}$); 7.11 (br, 3H, *H*-P$_{(Ar)}$, *H*$_3$); 7.05 (br, 1H, *H*$_8$); 6.92 (br, 2H, *H*-P$_{(Ar)}$); 4.15 (br, 1H, C*H*$_{2a'}$); 3.82 (br, 1H, C*H*$_{2a}$); 3.09 (s, 3H, C*H*$_{3A}$); 2.31 (br, 3H, C*H*$_{3y}$); 1.94 (s, 3H, C*H*$_{3B}$); 1.60 (br, 3H, C*H*$_{3x}$). ^{31}P NMR ($C_2D_2Cl_4$, $T = 233$ K): δ 30.3 ($^1J_{PtPav} = 4413$ Hz).

X-ray Data Collection and Structure Refinement. Air-stable, red-yellow crystals of [Pt(dmphen){$CH_2C_6H_4P$(*o*-tolyl)$_2$-*κC,P*}]-BArf(**10**), suitable for X-ray diffraction, were obtained by slow diffusion of cyclohexane into a concentrated dichloromethane solution of the complex. A crystal of **10** was mounted on a Bruker SMART diffractometer, equipped with a CCD detector, and cooled, using a cold nitrogen stream, to 150(2) K for the determination of the unit cell, crystal symmetry, and for the data collection. The triclinic $P\bar{1}$ space group was later confirmed by the successful refinement, whereas the cell constants were refined, at the end of the data collection, with the data reduction software *SAINT*[36]. The experimental conditions for the data collections, crystallographics, and other relevant data are listed in Table 4 and in the Supporting Information. The collected intensities were corrected for Lorentz and polarization factors[36] and empirically for absorption using the *SADABS* program.[37]

The structure was solved by Patterson and Fourier methods and refined by full-matrix least squares,[38] minimizing the function $[\sum w(F_o^2 - (1/k)F_c^2]^2$ and using anisotropic displacement parameters for all of the atoms except the hydrogens. Some of the fluorine atoms of the BArf counter ions are disordered, as shown by their large amplitude motion. A disordered model, with fluorine atoms split in two different orientations, did not improve the R factors, thus the anisotropic (single-occupancy) model was retained. The contribution of the hydrogen atoms, in their calculated position, was included in the refinement, using a riding model (B(H) = $aB_{(C_{bonded})}$(Å^2), where $a = 1.5$ for the hydrogen atoms of the methyl groups and $a = 1.3$ for the others). No extinction correction was deemed necessary. The scattering factors used, corrected for the real and imaginary parts of the anomalous dispersion, were taken from the literature. All of the calculations were carried out by using *SHELX-97*,[39] *WINGX*,[40] and *ORTEP*[39] programs.

Variable-Temperature NMR Experiments. In a typical experiment, approximately 6 mg of the complex was dissolved in the appropriate deuterated solvent. When required, a controlled amount of a nucleophile (thioether) was added. The ^{1}H NMR spectrum was recorded in a sealed NMR tube over a temperature range depending on the rate of the fluxional motion. For **1**−**5**, the ^{1}H NMR spectra were recorded from 298 to 350 K in $C_2D_2Cl_4$. The rate of restricted rotation of the phosphane ligand P(*o*-tolyl)$_3$ around the Pt−P bond was evaluated from line-shape analysis of the resonances of the methyl protons CH_{3x}, CH_{3y}, and CH_{3z} of the *o*-tolyl groups. Either the aromatic protons H_4−H_7 or the methyl protons CH_{3A} and CH_{3B} of the phenanthroline were monitored and used for the line-shape estimation of the rate of dmphen flipping. The same criteria were applied to the study of the dynamic motion of ligands in the cyclometalated [Pt(dmphen){$CH_2C_6H_4P$(*o*-tolyl)$_2$-*C,P*}]X (X= PF_6, **6**; X = CF_3SO_3, **8**) complexes. Again, the signals of the aromatic protons H_4−H_7 and of the methyl protons CH_{3A} and CH_{3B} of the phenanthroline were monitored in the temperature range of 305−415 K in $C_2D_2Cl_4$ and used for the line-shape estimation of the rate of dmphen flipping. The much-faster rotation of the phosphine tolyl groups around the Pt−C$_{ipso}$(*o*-tolyl) bonds was monitored in

(36) BrukerAXS, *SAINT*, Integration Software; Bruker Analytical X-ray Systems: Madison, WI, 1995.
(37) Sheldrick, G. M. *SADABS*, Program for Absorption Correction; University of Göttingen: Göttingen, Germany, 1996.
(38) Sheldrick, G. M. *SHELX-97*, Structure Solution and Refinement Package; University of Göttingen: Göttingen, Germany, 1997.
(39) Farrugia, L. J. *J. Appl. Crystallogr.* **1999**, *32*, 837−838. (b) Farrugia, L. J. *J. Appl. Crystallogr.* **1997**, *30*, 565.
(40) *SCIENTIST*; Micro Math Scientific Software: Salt Lake City, UT.

a lower range of temperature (from 225 to 300 K) through both the changes of the methyl signals of the *o*-tolyl groups and those of the coordinated methylene group. The exchange rates were calculated using the computer program *gNMR 4.0*.[20] The activation parameters $\Delta G^{\ddagger}$ (at 333 K), $\Delta H^{\ddagger}$, and $\Delta S^{\ddagger}$ were derived from a linear regression analysis of the Eyring plots.

Cycloplatination ^{1}H NMR Kinetics. The kinetics of phosphane metalation on the complex [Pt(Me)(dmphen)(P(*o*-tolyl)$_3$)]CF_3SO_3 (**3**) was monitored by ^{1}H NMR spectroscopy. In a typical experiment, 10.0 mg of **3** were dissolved in 1.0 mL of tetrachloroethane-d_2 and placed in a sealed ^{1}H NMR tube. NMR spectra were recorded at regular intervals until the completion of the reaction at a constant temperature. Selected peaks (e.g., Pt−CH_3 of the starting **3** or Pt−CH_2 of the product **8**) were integrated, the values obtained were normalized and plotted versus time, showing exponential curves for the change with time of the molar fraction F of the reacting **3** or the product **8.** The first-order rate constant k_c, s^{-1} was obtained from the nonlinear regression analysis of the equation $F = c_1 + c_2 \exp(-k_c t)$ with c_1, c_2, and k_c as the parameters to be optimized. The variable-temperature rate constants, were fitted to the Eyring equation to derive the activation parameters.

Spectrophotometric Kinetics. Cyclometalation kinetics of **4** were followed by conventional spectrophotometry by repetitive scanning of the spectrum at suitable times in the range 320−220 nm. The reaction was started by dissolving a suitable amount of **4** in $C_2H_2Cl_4$ in a 1 cm quartz cell placed in the thermostated cell compartment of a JASCO V-560 UV−vis spectrophotometer. The reactions went to completion, the final spectra being identical with that of solutions of authentic samples of **9**. Rate constants were evaluated with the *SCIENTIST*[41] software package by fitting the absorbance/time data to the exponential function $A_t = A_{00} + (A_0 - A_{00}) \exp(-k_{obs}t)$. Rate constants are reported in Table SI2 in the Supporting Information as average values from five to seven kinetic runs.

Acknowledgment. We are grateful to the Ministero dell'Università e della Ricerca Scientifica e Tecnologica (MIUR), PRIN 2004, and to the University of Messina, PRA 2003, for funding this work.

Supporting Information Available: Figure showing the catalytic effect of Me_2S on the rates of dmphen flipping on **5**. Tables giving counteranion, solvent, and temperature dependence of primary kinetic data for **1**−**10**. Extended Tables of crystallographic data, coordinates, ADP's and bond distances, bond angles, and torsion angles as a CIF file. This material is available free of charge via the Internet at http://pubs.acs.org.

IC701396J